Characterization of Chaos: a New Fast and Effective Measure

Ioannis V. Sideris[1]
[1] *Department of Physics, Northern Illinois University, DeKalb, IL 60115, USA*

A new technique of characterization of the regular or chaotic nature of dynamical orbits has been discovered. It takes advantage of morphological and dynamical properties of orbits, and is very effective for at least time-independent systems of two degrees of freedom. The new technique was initially designed with time-dependent and N-body systems in mind. For this reason one of its main goals is to provide straightforward information about the transient chaos associated with such regimes. Equally important is the distinction it can make between sticky and wildly chaotic epochs during the evolution of chaotic orbits. Its most important advantage over the existing methods is that it can characterize an orbit using a very small number of orbital periods. For these reasons the new method is extremely promising to be useful and effective in a broad spectrum of disciplines.

PACS numbers: 45.10.-b, 52.25.Fi, 29.27.-a

I. INTRODUCTION

The characterization of the periodic or chaotic nature of dynamical orbits has been an important issue in many different disciplines. Correct characterization can contribute to critical understanding and subsequent intuition about the dynamics of a system. A number of techniques have been contrived to pursue the problem [1] [2] [3] [4]. Most of them are based either on the convergence of a measure, with typical example the Lyapunov exponents [5], or a frequency analysis scheme, like Laskar's method [6].

There is no doubt that these methods have proven valuable in the past and they can provide critical information. Still they have limitations. The typical complaint is that they require long evolution times to provide reliable results. The best methods usually need at least tens or even hundreds of orbital periods to provide confident characterizations. This means that in contexts like galactic dynamics, or even worse, charged-particle beams, where the evolution time is relatively short, these methods may be problematic. Lots of researchers have achieved serious breakthroughs in order to address this problem [1] [2] [3] [6], but generally it still stands.

A second problem is that the current methods have not been created by design to distinguish between the sticky [7] [8] and the wildly chaotic epochs of a chaotic orbit. It is well known that a chaotic orbit may stay trapped close to a regular island for a long time, and then escape into a broader chaotic sea where it can move without constraints. Such escapes are associated with motion through cantori (in two dimensions), or in Arnold's web (in three or more dimensions). The need for distinction between these two regimes and the computation of diffusion times has appeared in several contexts [9], including the structure and evolution of galaxies [10].

A third, more complex, problem is related to the phenomenon of transient chaos, which appears in time-dependent systems. In these regimes the time-dependence may cause an orbit to move from regular into chaotic (and vice versa) several times during its evolution [11]. The established methods can give information in an average-like manner, but they have not been designed to easily provide additional information about when these transitions happen. Extraction of this information using the existing measures, although not impossible, is usually tedious to achieve.

A new method has been devised that attempts to address all these problems. It is based on a new approach only loosely connected to the previous techniques. In Section II the new technique is presented for a typical example. In Section III advantages and disadvantages of the new method, as well as plans for future work are discussed.

II. DESCRIPTION OF METHOD

A random set of 500 initial conditions, with energy 0.125, were integrated in the Hénon-Heiles potential [12]:

$$V(x,y) = \frac{1}{2}(x^2 + y^2 + 2x^2y - \frac{2}{3}y^3) \qquad (1)$$

Their orbital data y, v_x, and v_y were recorded, in the typical Poincaré section fashion, when the orbits were crossing the plane y ($x = 0$). For convenience, hereafter, these orbital data series y, v_x, and v_y (recorded when $x = 0$) will be called "signals" or "time-series." The largest Lyapunov exponent of every orbit was also computed for comparison.

When one plots the Poincaré section of an orbit, morphological patterns emerge. One can visually identify regions of regularity and chaos. The periodic patterns of regular orbits on a Poincaré section are consequences of the existence of global and local integrals of motion, associated with underlying dynamical symmetries. When the number of underlying global and local symmetries is smaller than the number of degrees of freedom of the system, chaotic motion emerges and the periodic patterns are absent.

Similarly one can identify an obvious difference between regular and chaotic orbits when he/she plots the points that comprise the recorded time-series *without* the

lines that connect them (Figs. 1 and 2). For regular orbits there are similar morphological patterns that succeed each other (Fig. 1). On the other hand morphological patterns are absent in chaotic orbits in the strict, obvious way they exist in regular orbits (Fig. 2). However, one can still recognize some loose repetition in parts of a chaotic time-series. It is this loose repetition that often corresponds to a sticky epoch of a chaotic orbit. A striking observation is that the signal of a chaotic orbit provides hints about its evolutionary history, revealing visits to a number of stochastic regions, which are characterized by different properties.

One may want to notice that a signal reveals not just spatial patterns (like a Poincaré section does), but *spatiotemporal* patterns instead. The difference is important. Not only should one search for order in a restrained region of the phase space (where only positions and velocities are involved), but one also has to investigate whether the recorded points repeat themselves in an ordered way in time. For example if one shuffles the recorded times of the data points of a regular orbit, its Poincaré section will look exactly the same, because the Poincaré section is a plot of the position and velocity variables only and does not involve time. On the other hand, when the recorded times of the data are shuffled, the plot of the time-series points will show no patterns, exactly because time is involved in this plot. Therefore, the patterns one recognizes in a signal are not just spatial/morphological but spatiotemporal in nature. The spatial data do relate to and reveal part of the dynamics, but since signals involve both space and time one can hope that they may associate with dynamics even more precisely.

Several questions immediately arise: What is an effective algorithm to identify spatiotemporal, sequential patterns? How does analysis based on sequential patterns compare to the characterization of orbits by established measures, like Lyapunov exponents? How can one use the loose patterns in the signals of the chaotic orbits to identify their epochs of stickiness? Are sequential patterns always adequate for characterization of the nature of an orbit?

To zeroth order the sequential patterns of signals can be defined in a rather straightforward manner. Generally, a sequential pattern exists in a signal when, starting at a point y_n of a signal, the conditions $|y_k - y_n| < \epsilon$, and $|y_{k+1} - y_{n+1}| < \epsilon$, ..., and $|y_{2k-n-1} - y_{k-1}| < \epsilon$, (with ϵ a small number), are all true. What this means practically is that, k successive points in the signal almost repeat themselves sequentially. Later it will be addressed what "almost" means and how ϵ can be computed effectively.

A generalization of the aforementioned inequality condition to all three available signals y, v_x, and v_y, was applied to search for sequential patterns in the evolution of orbits in the Hénon-Heiles potential. Specifically, a sequential pattern of order k, exists when $|y_k - y_n| < \epsilon$ or $|v_{xk} - v_{xn}| < \epsilon$ or $|v_{yk} - v_{yn}| < \epsilon$, and $|y_{k+1} - y_{n+1}| < \epsilon$ or $|v_{xk+1} - v_{xn+1}| < \epsilon$ or $|v_{yk+1} - v_{yn+1}| < \epsilon$, ..., and $|y_{2k-n-1} - y_{k-1}| < \epsilon$ or $|v_{x2k-n-1} - v_{xk-1}| < \epsilon$ or $|v_{y2k-n-1} - v_{yk-1}| < \epsilon$. (It has to be mentioned that since the time-series can be considered a map, the discussion directly applies to maps too.)

Every pattern corresponds to a time segment of the orbital data. After all the existing patterns are identified, the union of their corresponding time segments is computed. If this union spreads over the whole evolution time of the orbit, the orbit is characterized as regular, otherwise it is characterized as chaotic (Fig. 3).

The same scheme is capable of recognizing loose sequential patterns in chaotic orbits. These patterns are associated with the time a chaotic orbit spends in a sticky regime. Intuitively one expects there should be some underlying near-symmetries which characterize the orbit when it is sticky, and they are reflected in the existence of loose patterns. When only a part of a signal has loose patterns, it is identified as sticky chaotic; the rest is identified as wildly chaotic (Fig. 3).

Although an intelligent choice of ϵ can be made without employing a rigid scheme, that could lead to confusion. A relatively more rigid technique can be formulated. Assume that one wants to identify the sequential patterns of an orbit and determine their union for different values of ϵ, starting at zero. For an individual orbit the first pattern appears at some $\epsilon = a_0$. As ϵ increases the union becomes larger and eventually at some $\epsilon = a_1$ it spreads over the whole evolution time. If one plots the union of the time segments associated with patterns versus ϵ, a striking observation can be made. The slope of the curve for a typical regular orbit is very steep, while for a chaotic orbit it is usually much shallower (Fig. 4). If one computes the maximum of a_1 values achieved by the orbits with very steep slopes one can determine a value for the ϵ to serve as the criterion in the algorithm for the distinction between sticky and wildly chaotic epochs of chaotic orbits.

It has to be stressed here that an exact distinction between the sticky and the wildly chaotic regions of the phase space may not be possible. The sticky regime moves in a continuous way into the wildly chaotic regime and gradually disappears, while the stochastic sea dominates. Therefore the aforementioned computation of the value of ϵ, which can serve as a criterion for distinction between the two regimes, is only a suggestion, and different researchers may treat the problem differently. Still the suggested scheme seems to give sensible results.

Having established the largest value of a_1 value for a sample of regular orbits one may apply this criterion to the chaotic orbits the way it appears in Fig. 5. The parts of a chaotic orbit that have patterns (sticky) are on the left of this criterion line, and the ones that do not have any patterns are on the right (wildly chaotic). It has to be noted here that it may be possible to take advantage of the information included in Fig. 5 and connect it to diffusion times of sticky chaotic epochs, which will be part of future investigation and design.

The new method was able to identify easily the regular orbits, and for the chaotic orbits the sticky and wildly

chaotic parts (Fig. 6). It is obvious from the bottom left panel of that picture that the sticky regime does not separate abruptly from the wildly chaotic regime. Instead, there is an overlapping region between the two regimes. At larger distances from a regular island, the sticky region gradually becomes less dense and wildly chaotic behaviour starts emerging. Eventually the wildly chaotic regime dominates. This is rather natural; it reveals the existence of the continuum that describes the passing from stickiness to wildly chaotic behaviour.

Also it is interesting that two kinds of sticky epochs appear. The first is characterized by few long patterns and can be coined as "strong" sticky chaotic regions. However, it was possible to identify a second type of sticky epochs (usually not identified by other measures) which are characterized by many and short patterns, and they are located in the region of the main broken separatrices of the system and the main three hyperbolic points of the Hénon-Heiles potential. This type of sticky epochs will be called "weak." Although an arbitrary criterion that distinguishes between weak and strong sticky chaotic epochs is necessary, an intelligent choice is usually very straightforward.

How well do the characterizations by the new technique correlate to the largest Lyapunov exponents of the orbits? The answer is: amazingly well! The same initial conditions were integrated for different evolution times, from 25 differential equations (DE) units (corresponding to about 4 orbital periods) to 1200 DE units (corresponding to about 190 orbital periods). The number of the orbits of which the characterization agreed with their largest Lyapunov exponent was computed (Fig. 7). For evolution time bigger than 90 orbital periods the results agree remarkably: 99% of the orbits are characterized correctly. However the crucial point here is that between 10 and 90 orbital periods the success is in the 90% regime. Even for only 4 orbital periods (at least for the Hénon-Heiles potential) this method is able to identify correctly about 75% of the orbits!

This is a result of major importance. Although for short time evolution not all the orbits are characterized correctly (compared to their Lyapunov exponents), many of them are, and they are enough to provide adequate information for a crude view of the structure of the phase space (Fig 8). This was beyond the capabilities of the pre-existing methods. When the evolution time is longer not only this method agrees almost completely with the largest Lyapunov exponents but it also provides additional information about the sticky epoch of the chaotic orbits.

A comment is in order concerning the orbits that are not characterized correctly (about 10% of the orbits) when one uses data from only 10 orbital periods. These orbits are usually the very sticky ones that for the 10 orbital periods behave in a way very similar to that of a regular orbit (Fig 9). If one plots these orbits, their physiognomy is regular. However, dynamically they are chaotic, and they will escape to the stochastic sea later in their evolution. Nevertheless, when the evolution time of interest of a real system is as short as 10 orbital periods, one may be less interested in the dynamical nature of the orbits than in their physiognomy. This is something to be decided by the individual researcher in keeping with the nature of the problem.

How effective this method is can be seen if one plots the slope of the time-union curve (that appears in Figs. 4 and 5) versus the number of orbital periods. Steep slopes mean that the orbit is regular, while shallow slopes mean that the orbit is chaotic. In Fig. 10 examples for three typical regular and three typical chaotic orbits appear. It is obvious that the slopes converge to a value close to 90 degrees in about 10 orbital periods. On the other hand the chaotic orbits wander away from a steep angle and eventually converge to some value very different than 90 degrees.

Motion in a time-dependent potential may be characterized by transient chaos. Because the energy is not constant it is possible for an orbit to move from regular to chaotic and vice versa. In a time-dependent regime the described method can recognize when the orbit has repetitious epochs (regular) and when it does not. When repetitious patterns do not emerge the epoch is usually chaotic but it may also be regular but so short-lived that patterns did not have enough time to form. To this extent this method is able to distinguish automatically between the two regimes without any extra effort or analysis. In this sense it can be valuable to investigators interested in time-dependent systems.

The toy model used as a first application to a time-dependent regime was the Plummer potential plus a time-dependent sine perturbation of strength m_0 [11].

$$V(x,y) = -\frac{1}{\sqrt{1+x^2+y^2+z^2}} - \frac{m_0 \sin(\omega t)}{\sqrt{1+x^2+a^2y^2+z^2}} \tag{2}$$

with $a^2 = 1.1$ and $\omega = 0.5$.

The same 100 initial conditions were evolved in this potential for four different values of m_0. Then the orbital data were searched for repetitive patterns. It was found, as expected, that as the perturbation increases the number of orbits that stay regular throughout the whole evolution decreases (Fig. 11). Most orbits become chaotic and a small halo appears. What is striking however is that there is a repetitive region in the phase space which is located in the middle plane (axis y). When a particle finds itself in that region it will follow an ordered motion. This kind of information could not be extracted easily with previously available measures.

III. DISCUSSION AND CONCLUSIONS

The new method discussed in this paper has been carefully designed and engineered to provide a number of new pieces of information, which until now were either

not accessible at all, or at least were difficult to be computed. The advantages of this method are: (a) it applies to time-dependent as well as time-independent systems, (b) it applies to either maps or flows, (c) it is algorithmically straightforward and easily programmable, (d)it is neither computationally expensive nor memory intensive; it required less than two minutes to characterize 500 orbits evolved for 100 orbital periods (this is equivalent to about 200 points in the time-series) in a 3.2GHz AMD processor, (e) the characterization is computed on output data and not in real time during the evolution of an orbit, which can save considerable computer time, and (f) most importantly *it converges very fast* (for most of the orbits that was within about 10-15 orbital periods).

The main drawback of this method is that since it is based on the existence of patterns in the signals associated with Poincaré sections, it is not possible to provide a valid characterization before some patterns have already been formed. There may be ways to work around this problem in the future by taking advantage of other kinds of symmetries associated with the signal. It is true, however, that this problem did not appear (or did not seem to be very important at least) for the case of the Hénon-Heiles potential.

Also it has to be mentioned that the sequential-patterns method becomes computationally expensive for orbital data with many recorded points, like the the ones in celestial mechanics, or in storage rings in accelerators. However, in these contexts one may be in the position to trust the results from the analysis of the first few hundreds of points. Still there could be cases for which careful analysis of all the points is necessary. Then parallelization of the algorithm is required and this appears to be feasible.

The immediate future plans are to (1) solve the aforementioned problems, and (2) generalize this method to systems of three degrees-of-freedom as well as N-body systems. There the time-series may be more complicated because a bigger number of frequencies may characterize the motion. Then one may need to define and include a small extra number of different patterns (other than sequential). It will be of major physical interest to analyze more effectively, and thereby understand the time-dependent dynamics involved in many different systems, like for example beam dynamics in accelerators. Careful investigation may reveal underlying physics that was inaccessible or tediously accessible through previous techniques.

Acknowledgments

The author would like to express his deepest gratitude to his mentor Henry E. Kandrup. Henry's ethos, values, sense of humor, originality, knowledge, and intuition gave motivation and shape, to the ones who had the greatest luck to have met and/or worked with him. People like Henry are the "salt and pepper" of science and are literally irreplaceable. He is missed not only as a teacher but also, even more importantly, as a close and trusted friend.

This work was supported by the U.S. Department of Education under Grant No. P116Z010035, Energy under Grant No. DE-FG02-04ER41323, and Defense under Air Force Contract No. FA9451-04-C-0199.

[1] Contopoulos G. & N. Voglis, 1996, Spectra of stretching numbers and helicity angles in dynamical systems, Cel. Mech. Dyn. Astron. **64**, 1

[2] Skokos, C., 2001, Alignment indices: a new, simple method for determining the ordered or chaotic nature of orbits, J. Phys. A**34**, 10029

[3] Froeschle, C., E. Lega, & R. Gonczi, 1997, Fast Lyapunov indicators. Application to asteroidal motion, Cel. Mech. Dyn. Astron., **67**, 41

[4] Contopoulos G., 2002, Order and Chaos in Dynamical Astronomy, Springer-Verlag, Berlin

[5] Benettin, G, L. Galgani, A. Giorgilli, & J.-M. Strelcyn, 1980, Lyapunov characteristic exponents for smooth dynamical systems and for Hamiltonian systems- A method for computing all of them. I -Theory. II - Numerical application, Meccanica, **15**, 9 and 21

[6] Laskar, J., 1990, The chaotic motion of the solar system - A numerical estimate of the size of the chaotic zones, Icarus, **88**, 266

[7] Contopoulos, G.: 1971, Orbits in highly perturbed dynamical systems. III. Nonperiodic orbits. Astron. J., **76**, 147

[8] Shirts R. B. & W. P. Reinhardt, 1982, Approximate constants of motion for classically chaotic vibrational dynamics: Vague tori, semiclassical quantization and classical intramolecular energy flow, J. Chem. Phys. **77**, 5204

[9] Kandrup, H. E., I. V. Pogorelov, & I. V. Sideris, 2000, Chaotic mixing in noisy Hamiltonian systems, M.N.R.A.S. **311**, 719

[10] Athanassoula, E., O. Bienyam, L. Martinet, & D. Pfenniger, 1983, Orbits as building blocks of a barred galaxy model, A&A **127**, 349

[11] Kandrup, H. E., I. M. Vass, & I. V. Sideris: 2003, Transient chaos and resonant phase mixing in violent relaxation, M.N.R.A.S. **341**, 927

[12] Hénon, M. & C. Heiles: 1964, The applicability of the third integral of motion: Some numerical experiments, Astron. J. **69**, 73

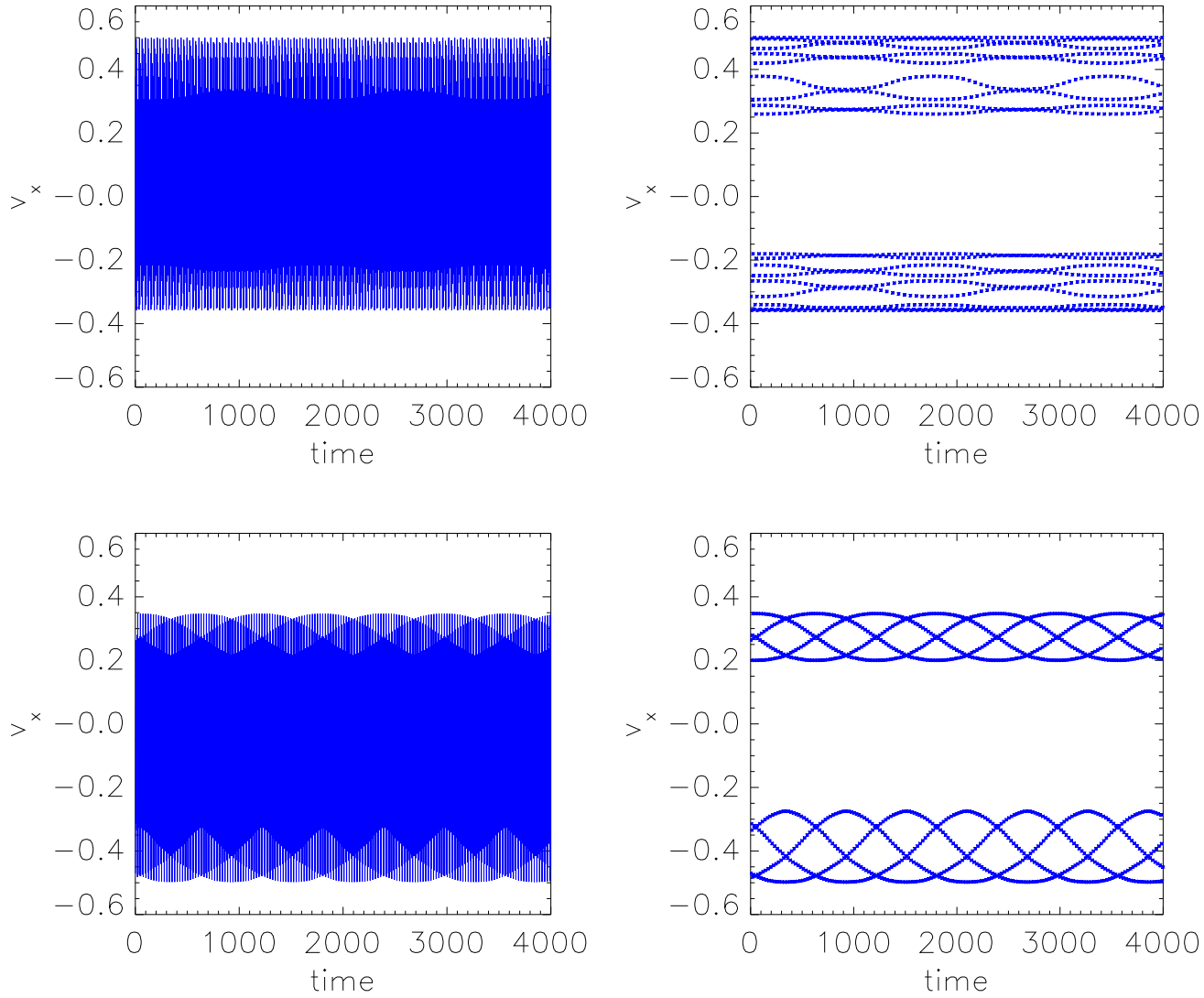

FIG. 1: Examples of the signals of the velocity v_x for two typical regular orbits evolved in the Hénon-Heiles potential (Eq. 1). The left panels show the recorded points with the lines that connect them. The right panels show the same signals but without the connecting lines between the points. It is obvious that repetitive patterns emerge.

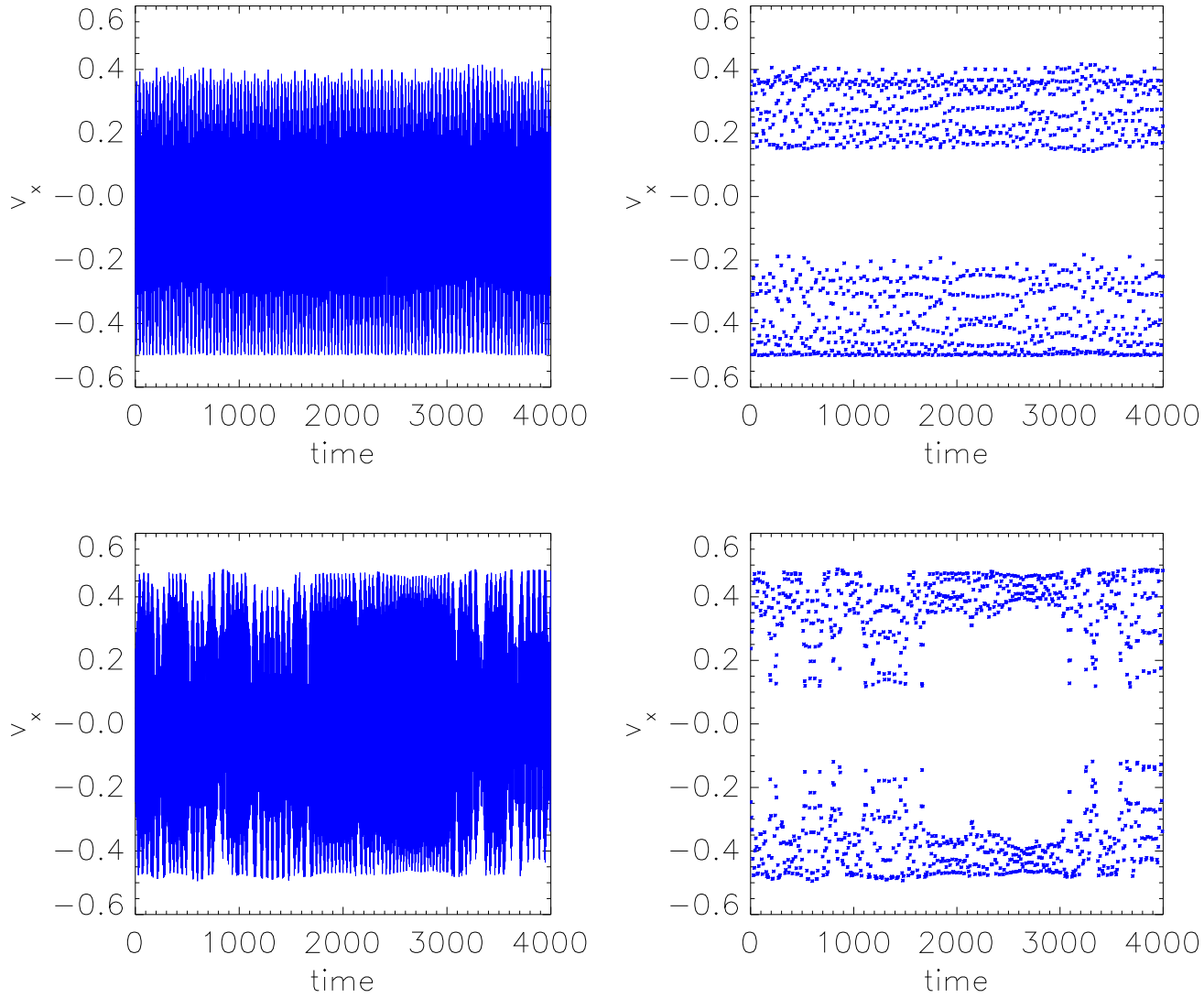

FIG. 2: Same as in Fig. 1 but for chaotic orbits. There are no patterns in the strict obvious sense that appear for regular orbits.

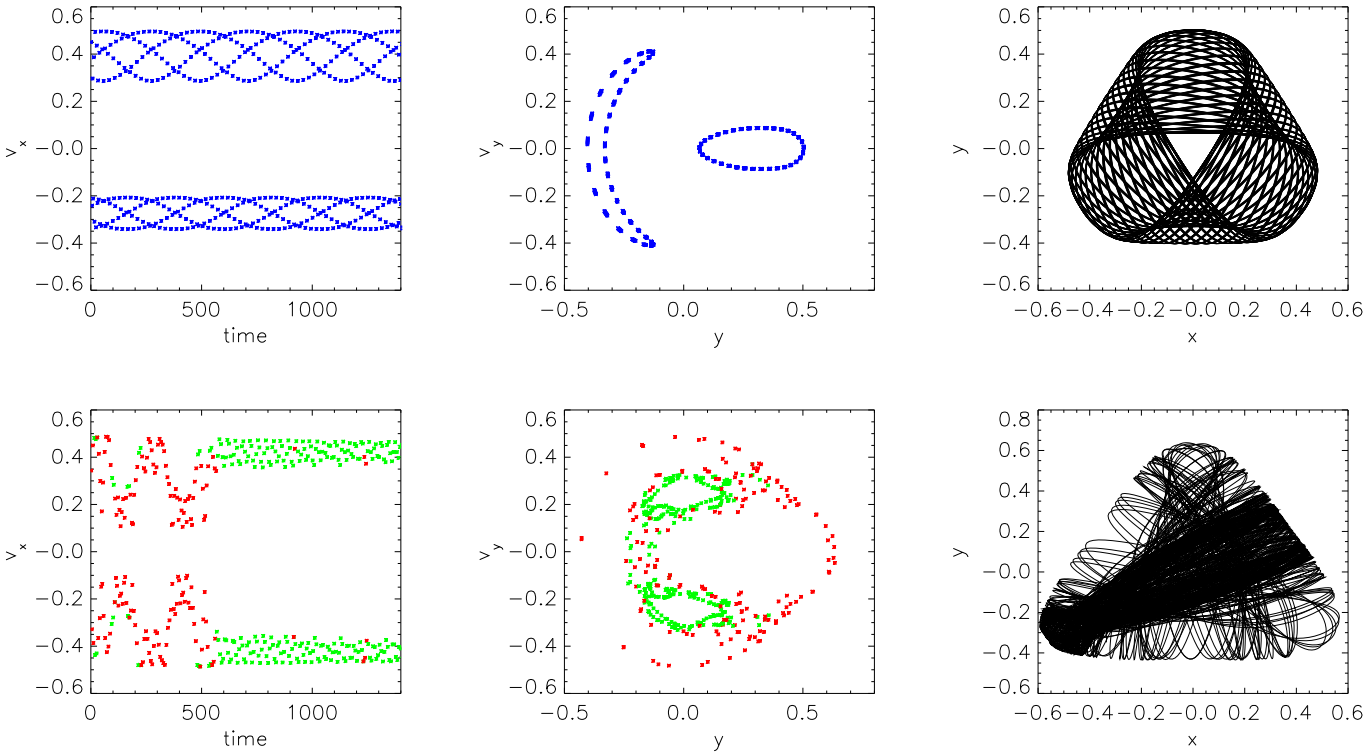

FIG. 3: Top left panel: the v_x signal of a regular orbit evolved in the Hénon-Heiles potential (Eq. 1). The algorithm identifies the patterns in these signals and the time segment that correspond to each pattern. The union of these time segments spreads over the whole evolution time; therefore, this orbit is characterized as regular. Top middle panel: the Poincaré section of this orbit. Top right panel: a plot of the orbit. Bottom right panel: the v_x signal of a chaotic orbit evolved in the same potential. There are parts with no repetition (red dots), and parts with loose repetition (green dots) which correspond to sticky epochs of the evolution. Bottom middle panel: the Poincaré section of the orbit. The green dots correspond to the green (sticky) dots of the signal. It is obvious that the green dots are localized in a sticky region. Bottom left panel: plot of the orbit.

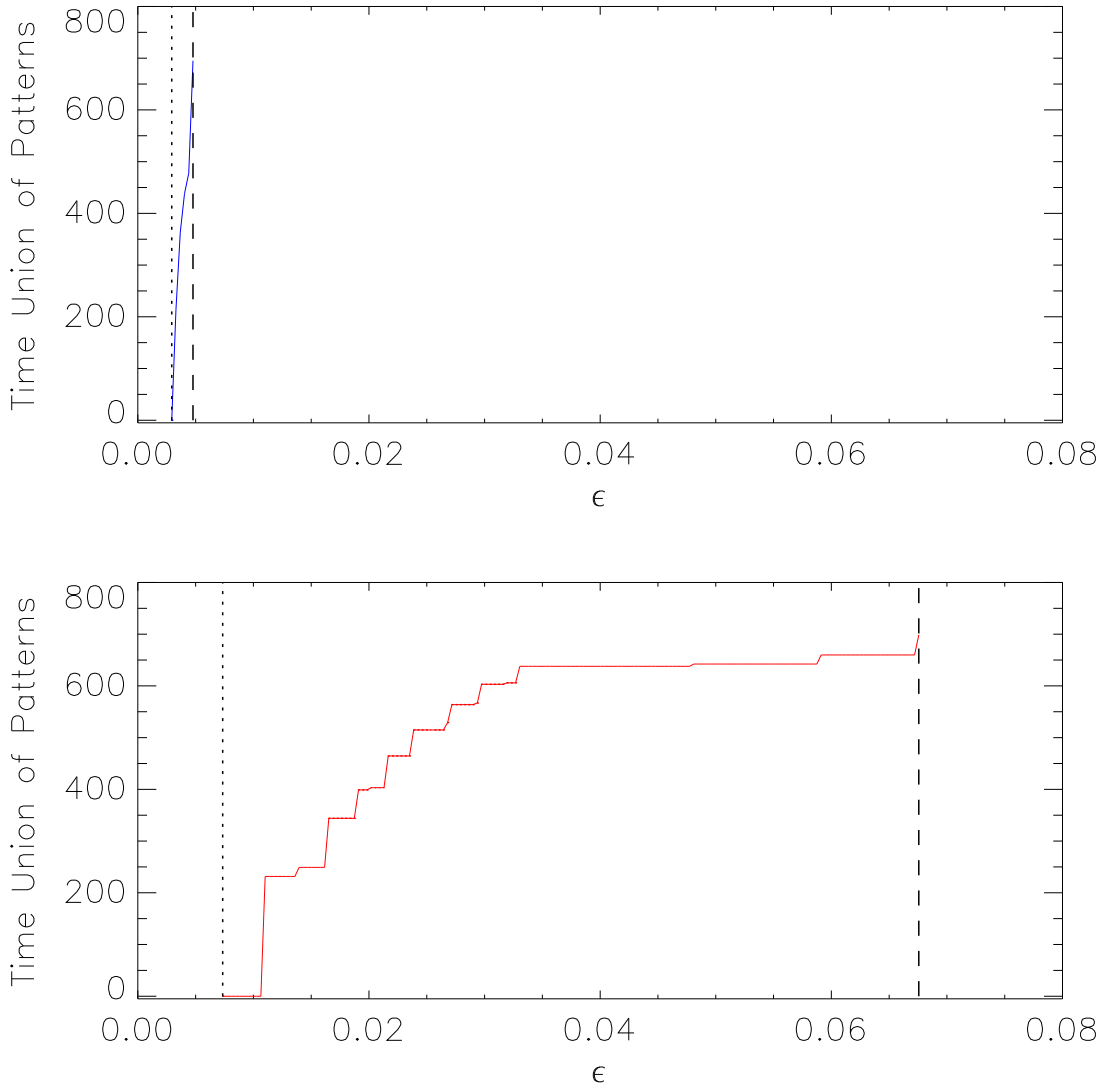

FIG. 4: The time-union of patterns versus ϵ for a regular orbit (top panel) and a chaotic orbit (bottom panel) evolved in the Hénon-Heiles potential (Eq. 1). The dotted line signifies the smallest $\epsilon = a_0$ for which a pattern appears while the dashed line signifies the $\epsilon = a_1$ for which the time-union of patterns equals the whole evolution time, which in this example was 700 DE units (about 100 orbital periods).

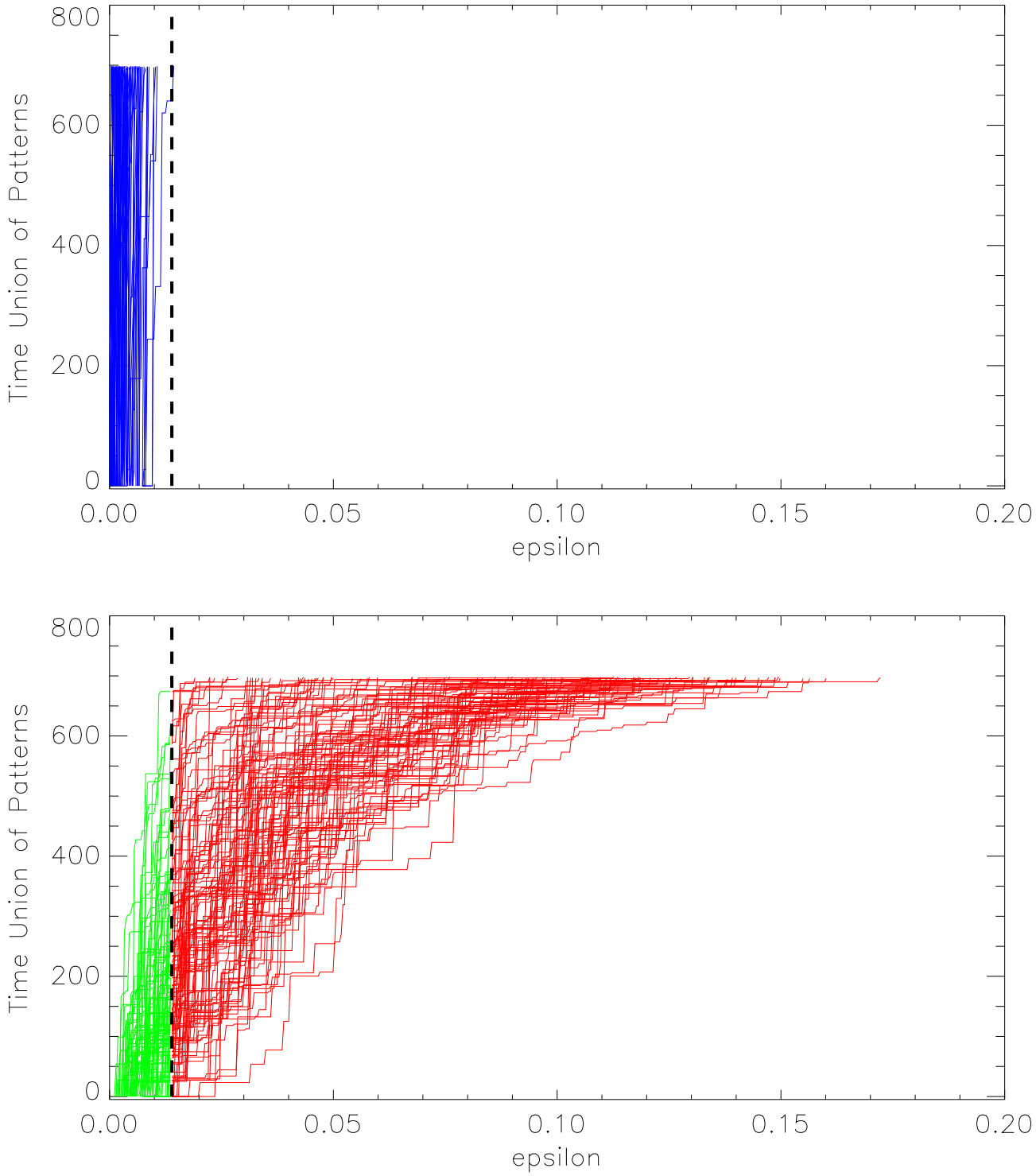

FIG. 5: Union of the time-segments associated with patterns for several orbits evolved in the Hénon-Heiles potential (Eq. 1). Top panel: regular orbits. Bottom panel: chaotic orbits. The dashed line signifies the value of the biggest ϵ achieved by any orbit with slope of time-union bigger than 89 degrees. Extending this line into the chaotic orbits plot can serve as a criterion for distinguishing between sticky (green) and wildly chaotic (red) epochs of chaotic orbits.

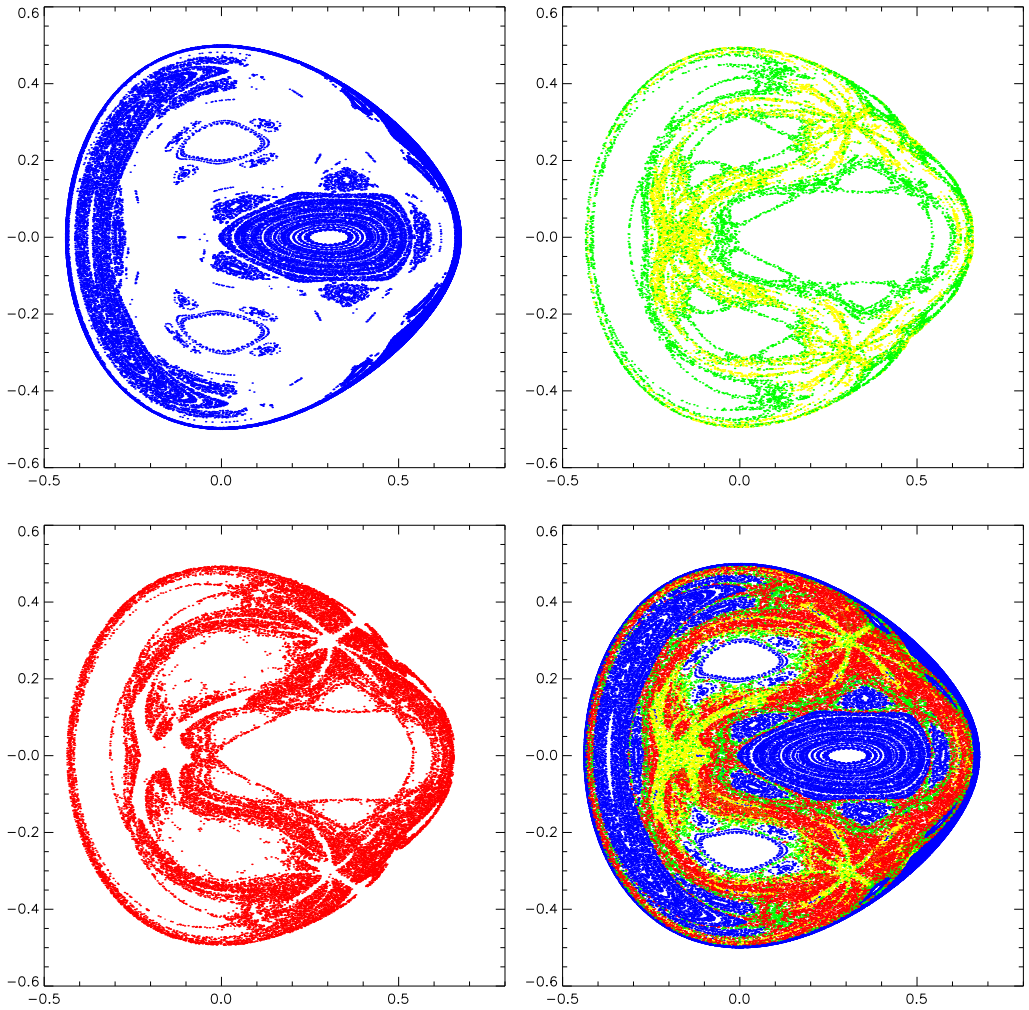

FIG. 6: Phase space of the Hénon-Heiles potential (Eq. 1) for a sample of 500 orbits of energy 0.125, integrated for about 100 orbital periods. Top left panel: regular orbits. Top right panel: strong sticky epochs of chaotic orbits are green while weak sticky epochs are yellow. Bottom left panel: wildly chaotic epochs of chaotic orbits. Bottom right panel: all orbits.

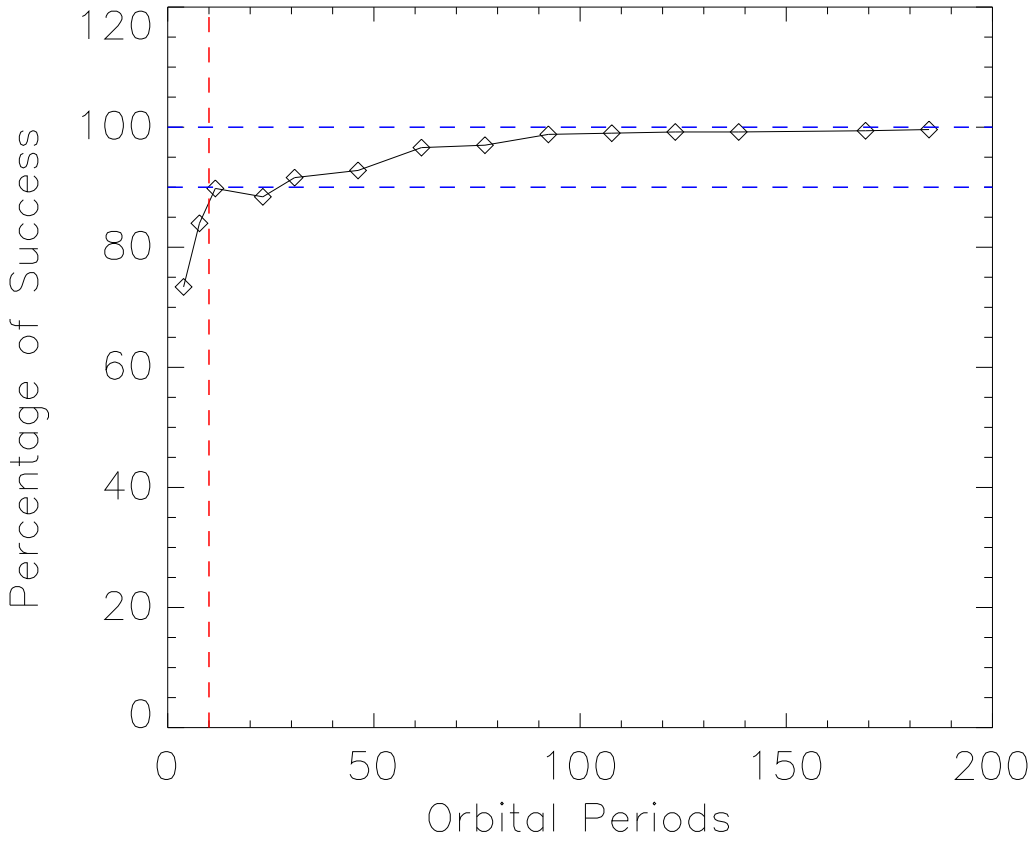

FIG. 7: The success percentage for 500 initial conditions evolved in the Hénon-Heiles potential (Eq. 1) for a number of different evolution times, was computed by comparing how many of the orbits agree with the characterization provided by their largest Lyapunov exponents.

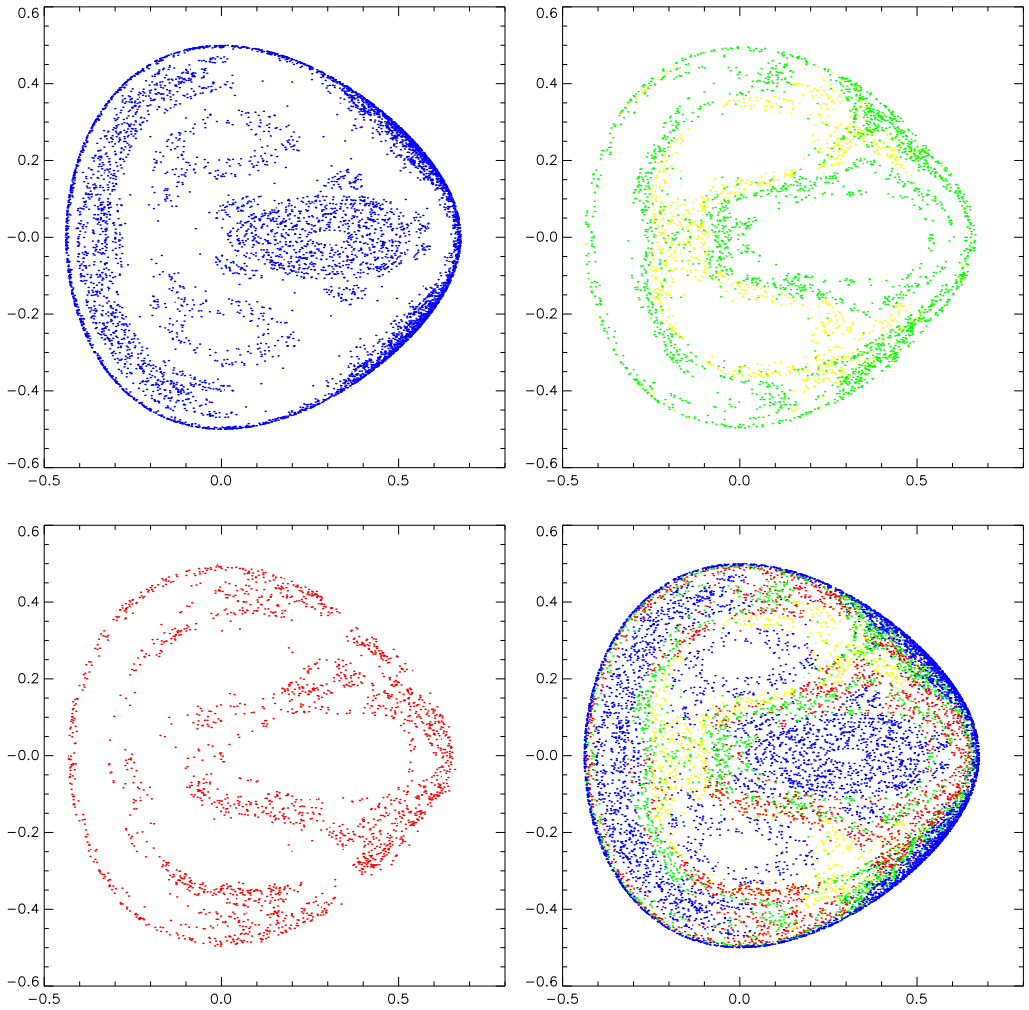

FIG. 8: Phase space of the Hénon-Heiles potential (Eq. 1) for a sample of 500 orbits of energy 0.125, integrated for only 10 orbital periods. Top left panel: regular orbits. Top right panel: strong sticky epochs of chaotic orbits are green while weak sticky epochs are yellow. Bottom left panel: wildly chaotic epochs of chaotic orbits. Bottom right panel: all orbits.

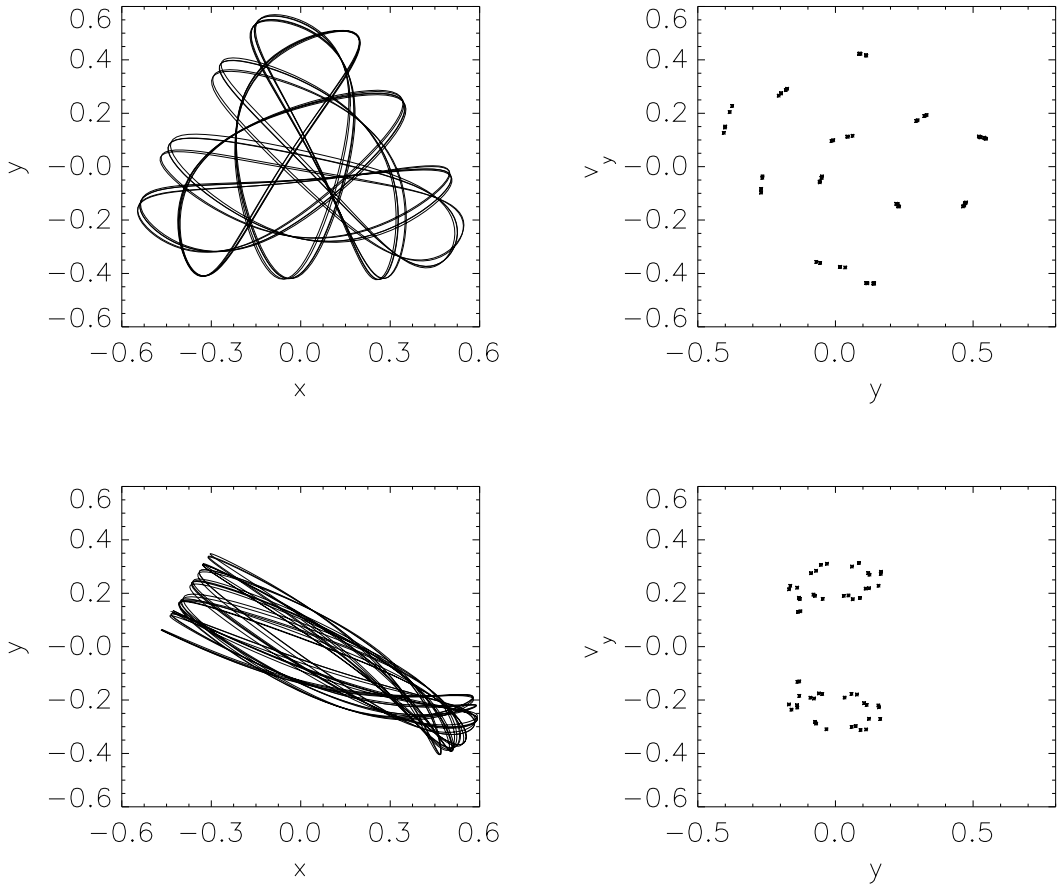

FIG. 9: Two examples of sticky orbits and their Poincaré sections, (evolved in the Hénon-Heiles potential (Eq. 1)), which are characterized as regular when the data of only 10 orbital periods are used. Later these orbits will escape to the stochastic sea.

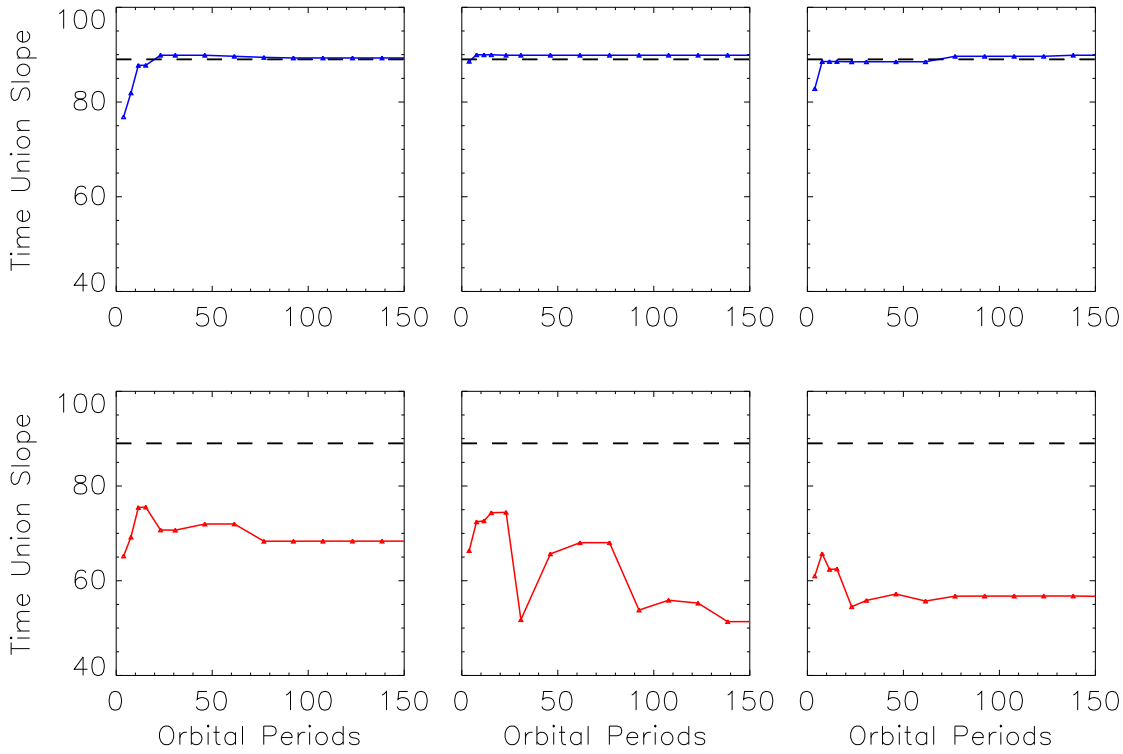

FIG. 10: Slope of time-union of patterns versus number of orbital periods. The top three panels correspond to typical regular orbits evolved in the Hénon-Heiles potential (Eq. 1). All three of them converge to a value close to 90 degrees (the dashed line is located at 89 degrees). The bottom three panels correspond to typical chaotic orbits evolved in the same potential. Their curves wonder well away from 90 degrees. The distinction is clear.

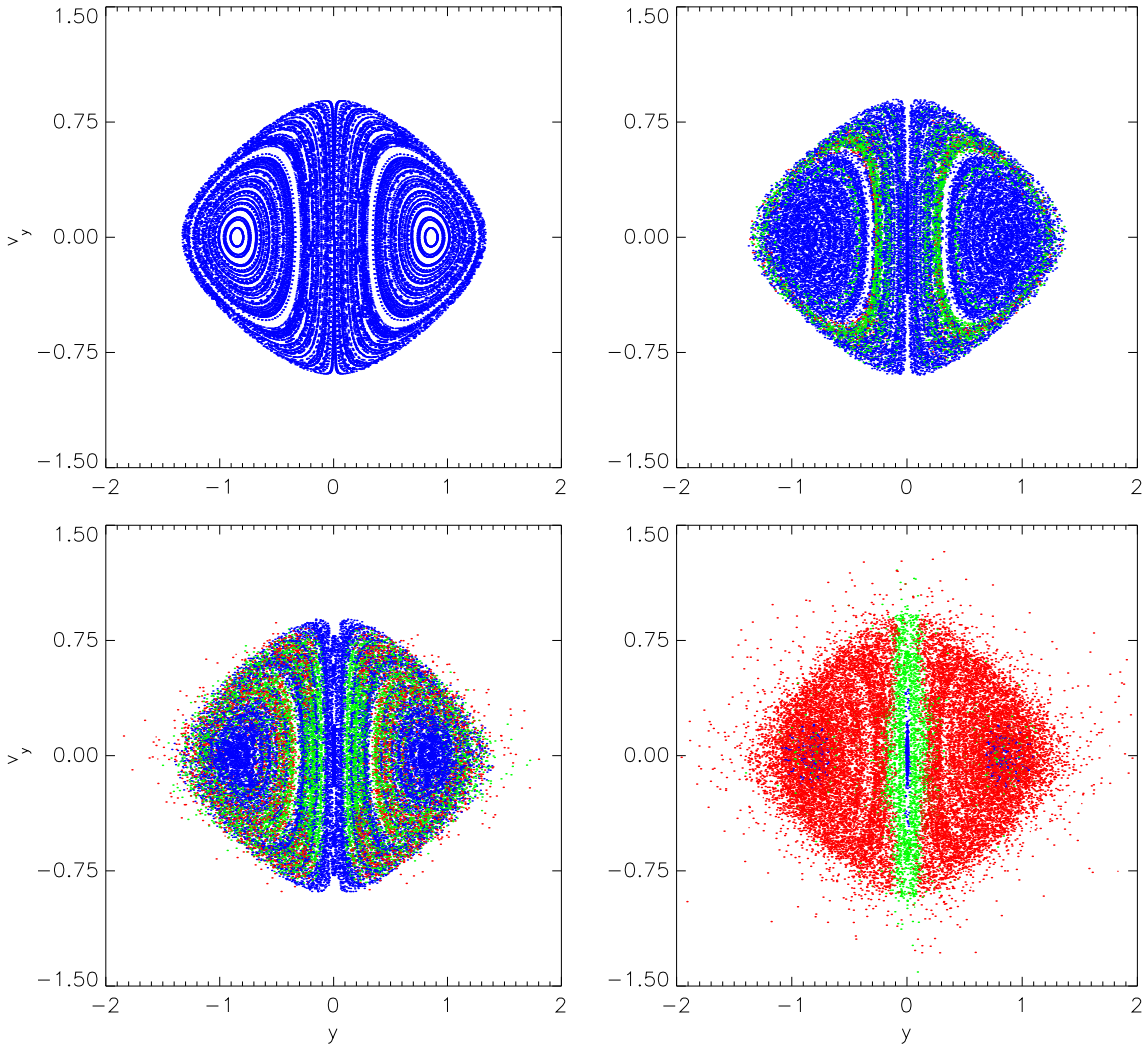

FIG. 11: Phase space of the Plummer plus time-dependent perturbation potential (Eq. 2) for a sample of 100 orbits, integrated for about 100 orbital periods (in average). Top left panel: perturbation $m_0 = 0$, all orbits are regular (blue). Top right panel: perturbation $m_0 = 0.10$. There is still a good number of orbits that stay regular throughout their whole evolution (blue), but some wildly chaotic epochs start appearing (shown in red). The algorithm distinguishes between the chaotic and the regular epochs of orbits that move from regular to chaotic and vice versa. The green parts show regular epochs of orbits that experienced some chaotic epoch(s) during their evolution (transient chaos). Bottom left panel: perturbation $m_0 = 0.17$. More chaotic epochs appear. Bottom right panel: perturbation $m_0 = 0.25$. Even more chaotic epochs appear. There is a green area that surrounds the y axis, which shows a regular epoch of transient orbits localized in a region of the phase space.